The microtubule cross-linker Feo controls the midzone stability, motor composition, and elongation of the anaphase B spindle in *Drosophila* embryos

Haifeng Wang, Ingrid Brust-Mascher, and Jonathan M. Scholey
Department of Molecular and Cell Biology, University of California at Davis, Davis, CA 95616

ABSTRACT **Chromosome segregation during anaphase depends on chromosome-to-pole motility and pole-to-pole separation. We propose that in *Drosophila* embryos, the latter process (anaphase B) depends on a persistent kinesin-5–generated interpolar (ip) microtubule (MT) sliding filament mechanism that "engages" to push apart the spindle poles when poleward flux is turned off. Here we investigated the contribution of the midzonal, antiparallel MT-cross-linking nonmotor MAP, Feo, to this "slide-and-flux-or-elongate" mechanism. Whereas Feo homologues in other systems enhance the midzone localization of the MT-MT cross-linking motors kinesin-4, -5 and -6, the midzone localization of these motors is respectively enhanced, reduced, and unaffected by Feo. Strikingly, kinesin-5 localizes all along ipMTs of the anaphase B spindle in the presence of Feo, including at the midzone, but the antibody-induced dissociation of Feo increases kinesin-5 association with the midzone, which becomes abnormally narrow, leading to impaired anaphase B and incomplete chromosome segregation. Thus, although Feo and kinesin-5 both preferentially cross-link MTs into antiparallel polarity patterns, kinesin-5 cannot substitute for loss of Feo function. We propose that Feo controls the organization, stability, and motor composition of antiparallel ipMTs at the midzone, thereby facilitating the kinesin-5–driven sliding filament mechanism underlying proper anaphase B spindle elongation and chromosome segregation.**

Monitoring Editor
Francis A. Barr
University of Oxford

Received: Dec 19, 2014
Revised: Feb 10, 2015
Accepted: Feb 13, 2015

INTRODUCTION

During mitosis, chromosomes are separated by chromosome-to-pole motility (anaphase A) and spindle elongation (anaphase B; Gadde and Heald, 2004; Gerdes *et al.*, 2010; Goshima and Scholey, 2010; Walczak *et al.*, 2010; Zheng, 2010; McIntosh *et al.*, 2012; Helmke *et al.*, 2013; Civelekoglu-Scholey and Cimini, 2014). The *Drosophila* embryo mitotic spindle assembles by a centrosome-directed mechanism that can be augmented by chromatin- and augmin-directed microtubule (MT) assembly (Hayward *et al.*, 2014) and then segregates chromosomes using both anaphase A and B (Brust-Mascher and Scholey, 2002; Maddox *et al.*, 2002). Whereas anaphase A depends on a combined kinesin-13–dependent pac-man-flux mechanism (Rogers *et al.*, 2004), we propose that anaphase B depends on a slide-and-flux-or-elongate mechanism in which the persistent sliding apart of interpolar microtubules (ipMTs) driven by kinesin-5 "engages" to push apart the spindle poles when poleward flux is turned off (Cole *et al.*, 1994; Kashina *et al.*, 1996; Brust-Mascher and Scholey, 2002, 2011; Brust-Mascher *et al.*, 2004, 2009; Cheerambathur *et al.*, 2007; van den Wildenberg *et al.*, 2008; Acar *et al.*, 2013; Wang *et al.*, 2013; Scholey *et al.*, 2014). Thus, in pre–anaphase B spindles, the outward sliding of ipMTs is balanced by the kinesin-13 (KLP10A)-catalyzed depolymerization of their minus ends at the poles, producing poleward flux (Rogers *et al.*, 2004), and the spindle maintains a steady length. After cyclin B degradation, however, the MT minus end–capping protein patronin (Goodwin and Vale, 2010) counteracts KLP10A activity at spindle poles to turn off ipMT minus end depolymerization so poleward flux ceases and the outwardly sliding ipMTs can now elongate the spindle

This article was published online ahead of print in MBoC in Press (http://www.molbiolcell.org/cgi/doi/10.1091/mbc.E14-12-1631) on February 18, 2015.

Address correspondence to: Jonathan M. Scholey (jmscholey@ucdavis.edu).

Abbreviations used: GFP, green fluorescent protein; ipMT, interpolar microtubule; MT, microtubule.

(Wang *et al.*, 2013). At the same time, ipMT plus ends display net growth and recruit MT-MT cross-linkers to assemble a more robust midzone, where the sliding motors act (Cheerambathur *et al.*, 2007). However, although the patronin-mediated suppression of KLP10A activity is sufficient to convert MT poleward flux to anaphase B spindle elongation, the function of this spindle midzone reorganization is unclear (Wang *et al.*, 2013).

The spindle midzone is a structure that assembles and self-organizes during anaphase and consists of a dense network of overlapping antiparallel ipMTs containing multiple motor proteins, regulatory molecules, and nonmotor microtubule-associated proteins (MAPs; Glotzer, 2009; Peterman and Scholey, 2009; Mitchison *et al.*, 2013). The assembly, organization, and function of this structure depend critically on members of the Ase1p (also known as PRC1 and MAP65) family of homodimeric nonmotor MAPs, which bind and diffuse along single MTs, cross-linking antiparallel MTs into bundles and accumulating cooperatively between pairs of overlapping antiparallel MTs. Like kinesin-5 motors, members of the Ase1p protein family display a significant preference for cross-linking MTs into antiparallel versus parallel orientations (Kapitein *et al.*, 2008; van den Wildenberg *et al.*, 2008), and this preference for antiparallel MT binding is unique among nonmotor MAPs (Duellberg *et al.*, 2013). Members of the Ase1p/PRC1 family specifically accumulate at the spindle midzone from anaphase to telophase and interact with motor proteins and other MAPs to facilitate their association with the midzone. Such motors and MAPs include kinesin-4 (Kurasawa *et al.*, 2004) and CLASP1 (Liu *et al.*, 2009) in mammalian cells and kinesin-5 (Khmelinskii *et al.*, 2009) and kinesin-6 (Fu *et al.*, 2009) in yeast. Thus Ase1p/PRC1 proteins play essential roles in spindle midzone organization and cytokinesis. Although the Ase1p-mediated recruitment of sliding motors has been shown to be crucial for anaphase B spindle elongation in yeast (Fu *et al.*, 2009; Khmelinskii *et al.*, 2009), in metazoan systems the interactions between Ase1p/PRC1 homologues and sliding motors and their roles in anaphase B spindle elongation are less well understood.

In this study, we took advantage of the *Drosophila* syncytial embryo system, which progresses through multiple mitoses without intervening cytokinesis, to investigate specifically the mitotic function of the Ase1p/PRC1 homologue, Feo. *Drosophila* contains two members of the Ase1p family, namely Feo, which plays essential roles in mitosis, and Sofe, which does not (and is not considered further here; Verni *et al.*, 2004). In previous studies, based on the analysis of mutants and RNA interference in fixed spermatocytes, neuroblasts, and cultured S2 cells, it was found that Feo is required to organize a robust central spindle in telophase, to target Polo kinase to the midzone (D'Avino *et al.*, 2007), and for contractile ring assembly and cytokinesis but it is dispensable for anaphase B (Verni *et al.*, 2004). Here we reevaluated the mitotic roles of Feo in living embryo spindles, focusing on its possible role in anaphase B. We find that Feo controls the stability and motor composition of the spindle midzone and is required for proper anaphase B spindle elongation and chromosome segregation in *Drosophila* embryos.

RESULTS

Feo accumulates at the anaphase B and telophase spindle midzone downstream of cyclin B degradation and cdk1 inactivation

We created transgenic flies expressing Feo–green fluorescent protein (GFP) or Feo-mCherry and used spinning disk confocal microscopy to investigate its dynamics throughout the cell cycle (Figure 1 and Supplemental Video S1). Feo-GFP localized to the cytoplasm during interphase and only faintly to mitotic spindles from prophase to metaphase, but increasing amounts of Feo-GFP accumulated at the spindle midzone from anaphase B onset, appearing as a bright equatorial band of increasing intensity perpendicular to the spindle long axis (Figure 1, A and B, and Supplemental Video S1). To determine whether this accumulation is cell cycle regulated, we injected the cdk1 inhibitor purvalanol into metaphase embryos expressing Feo-mCherry and the chromosome-associated kinesin-4, KLP3A-GFP, which normally translocates to the midzone during anaphase B (Kwon *et al.*, 2004). In wild-type embryo metaphase spindles, Feo localized faintly throughout the spindle, whereas KLP3A localized to chromosomes and weakly to spindles, as expected. After cdk1 inhibition, however, a premature metaphase spindle midzone is formed (Hu *et al.*, 2012), and both Feo-mCherry and KLP3A-GFP accumulated on this structure, mimicking their midzone localization during anaphase B and telophase in wild-type spindles (Figure 1C and Supplemental Video S2). Thus, in wild-type spindles, cdk1 inactivation promotes the assembly of a spindle midzone containing both Feo and KLP3A. We further confirmed that Feo accumulation occurs downstream of cyclin B degradation, because the injection of excess nondegradable cyclin B into embryos containing anaphase B spindles caused Feo-GFP to rapidly dissociate from the spindle midzone (Figure 1D and Supplemental Video S3). Thus Feo accumulation at the anaphase/telophase midzone is regulated by cyclin B degradation and cdk1 inactivation, concordant with previous work showing that the localization and function of human PRC1 and yeast Ase1p are also regulated by cell cycle–dependent phosphorylation (Zhu *et al.*, 2006; Fu *et al.*, 2009; Khmelinskii *et al.*, 2009).

Feo is essential for proper anaphase B spindle elongation and midzone organization

To examine the role of Feo in embryonic mitosis, we generated an antibody against Feo, which recognized a single band around 80 kDa by Western blotting against *Drosophila* embryonic extracts (Figure 1E), and tested its ability to inhibit Feo by microinjecting it into *Drosophila* syncytial embryos expressing fluorescent proteins. As expected (Brust-Mascher *et al.*, 2009; Wang *et al.*, 2013), injection of the anti-Feo antibody displaced Feo-GFP from spindles, forming fluorescent cytoplasmic immunoprecipitates, and caused a gradient of phenotypes with respect to spindle dynamics (Figure 1F and Supplemental Figure S1). To confirm the specificity of Feo inhibition, we also injected the anti-Feo antibody into flies expressing other GFP-tagged proteins, including kinesins-4, -5, -6, -8, -13, and -14, the MT tip tracker EB1, and the mitotic kinase polo, and observed that none were sequestered into cytoplasmic immunoprecipitates like those formed from Feo-GFP (unpublished data). This suggests that the anti-Feo antibody does not cross-react with and immunoprecipitate these other motors and microtubule-binding proteins.

To investigate the effect of Feo inhibition on spindle dynamics and chromosome segregation, we microinjected the anti-Feo antibody into flies expressing GFP-tubulin and red fluorescent protein (RFP)–histone (Figure 2). The anti-Feo–mediated inhibition of Feo function produced a striking gradient of mitotic defects from anaphase to telophase. In spindles proximal to the injection site, anaphase B spindle elongation was initiated but not sustained (e.g., s4 and s5 in Figure 2, A and B, right in E, and Supplemental Video S5), whereas distal spindles displayed normal anaphase B spindle elongation (e.g., s1 and s2 in Figure 2, A and B). In both cases, the midzone became progressively narrower until it disappeared in telophase (Figure 2, D and E).

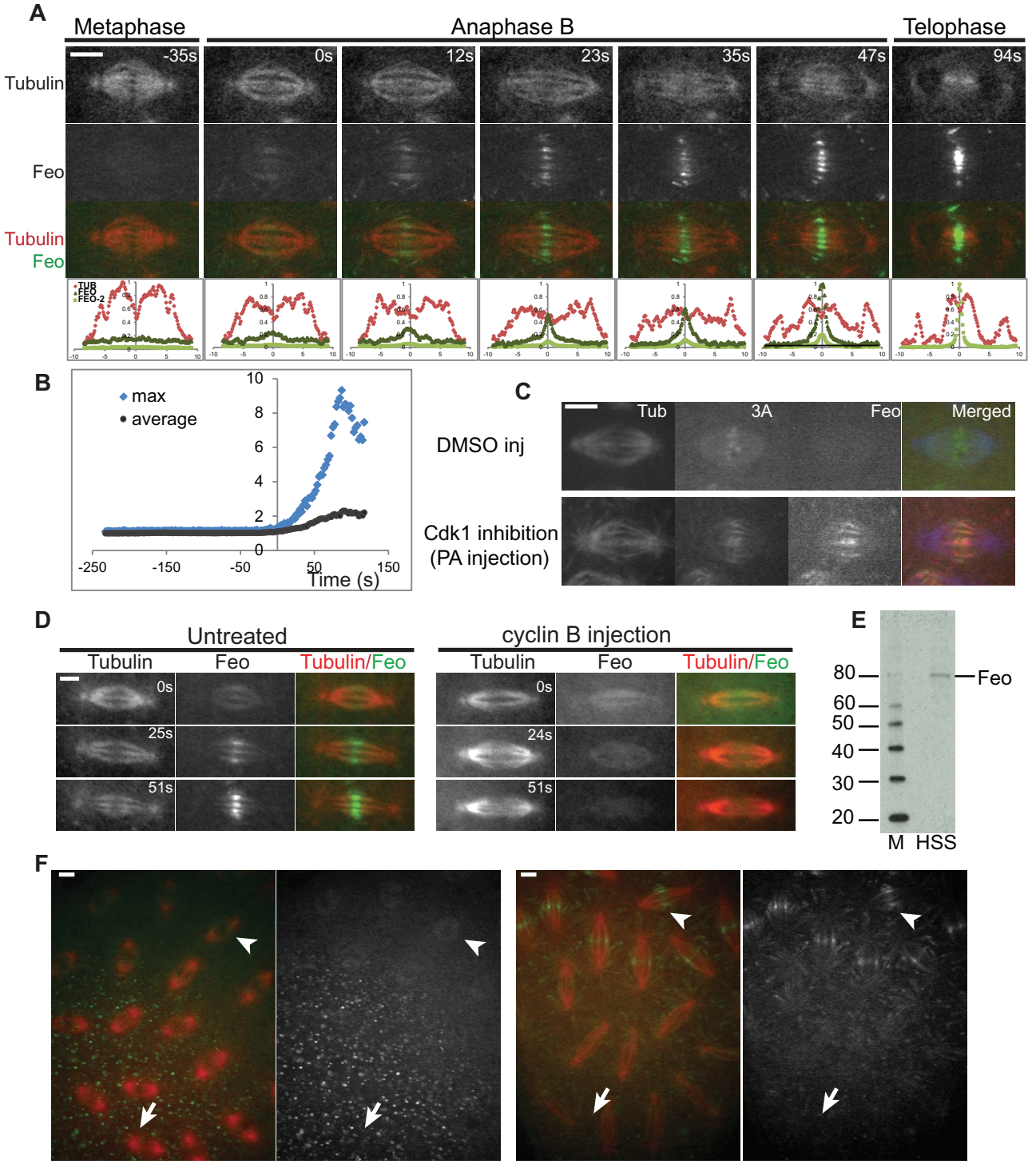

FIGURE 1: Cell cycle–dependent localization of Feo to the spindle midzone. (A) Feo accumulates at the spindle midzone from anaphase B through telophase. Living embryos expressing Feo-GFP (green in merged image) were injected with tubulin (red). 0 s, anaphase B onset. See Supplemental Video S1. Line scans show relative intensity along interpolar (ipMT) bundles. To calculate the relative fluorescence intensity, the minimum and maximum fluorescence intensity in all images were set to 0 and 1, respectively. Tubulin line scan is red, and Feo line scan is light green. To illustrate better the midzone accumulation of Feo at anaphase B, we also calculated the relative fluorescence intensity of Feo by setting the maximum fluorescence intensity during anaphase B to 1.0 (dark green line scan). (B) Example plot of fluorescence intensity of Feo-GFP vs. time at the spindle midzone normalized to average metaphase fluorescence. Blue, maximum intensity; black, average intensity calculated in a box surrounding the spindle midzone; 0 s, anaphase B onset. (C) The cdk1 inhibition by injection of the cdk1 inhibitor purvalanol caused KLP3A-GFP (green in merged) and Feo-mCherry (red in merged) to accumulate prematurely at the spindle midzone. Control was injected with dimethyl sulfoxide. Tubulin is blue in merged. See Supplemental Video S2. (D) Excess nondegradable cyclin B injection inhibited Feo accumulation at the anaphase B spindle midzone. See Supplemental Video S3. (E) Western blot of affinity-purified

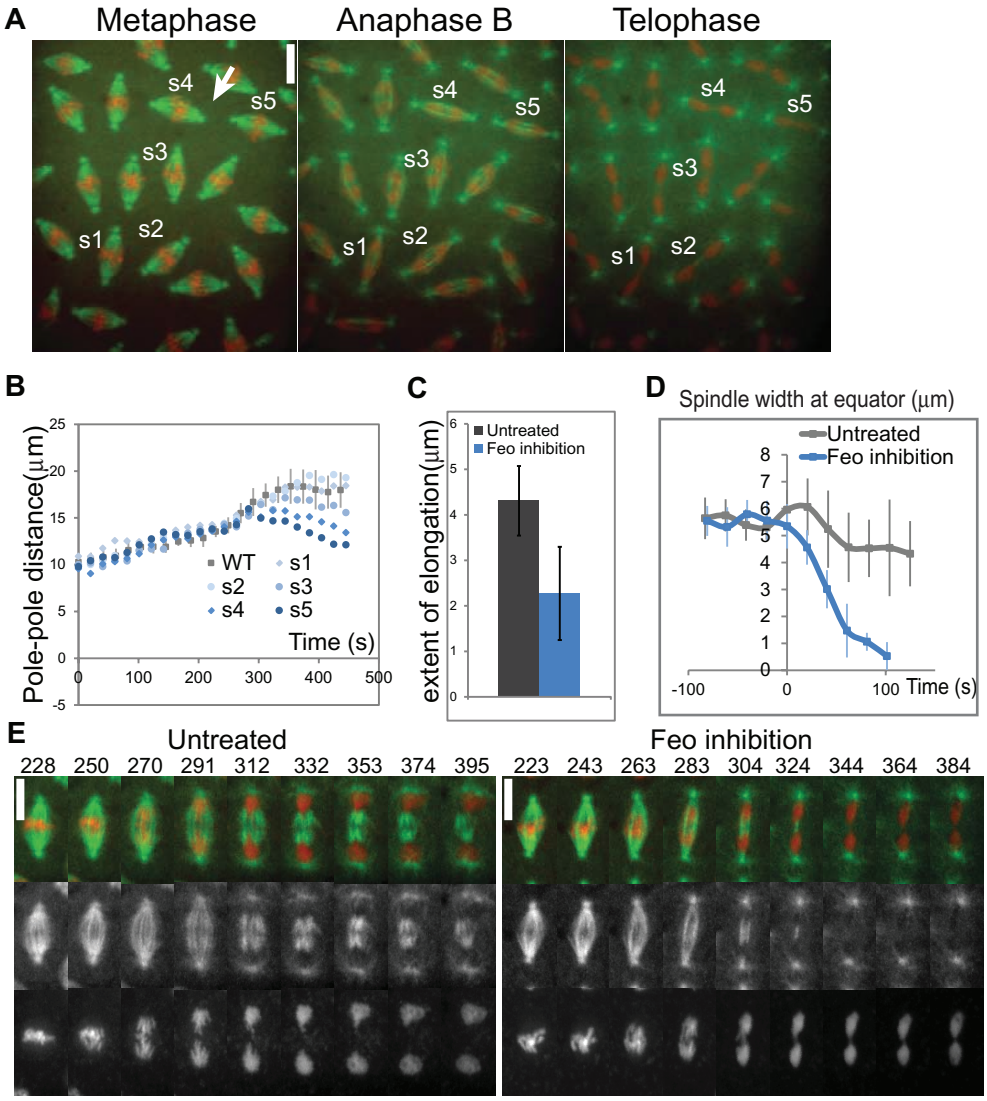

FIGURE 2: Feo inhibition caused defects in midzone stability and anaphase B spindle elongation in *Drosophila* embryos. Images (A) and plots of spindle length vs. time (B) for a representative embryo injected with anti-Feo (arrow) at nuclear envelope breakdown (NEB; 0 s) showing a gradient of phenotypes. Green, tubulin; red, histone. Close to the injection site (spindles 4 [s4] and 5 [s5] in A and B), spindles initiated anaphase B elongation but did not elongate to the full extent. In contrast, distal spindles (spindles 1 [s1] and 2 [s2] in A and B) displayed normal anaphase B spindle elongation. Repeated in >25 embryos. See Supplemental Videos S4 and S5. Bar, 10 μm. (C) Comparison of the extent of anaphase B spindle elongation in untreated and anti-Feo–injected embryos. $p = 1.009e\text{-}10$. (D) Plots of spindle midzone width vs. time in untreated and anti-Feo–injected embryos. 0 s, anaphase A onset. Averages of ≥6 spindles. (E) Representative spindle after Feo inhibition compared with control (untreated). Center row = MTs, bottom row = chromosomes, top row = double label MTs green, chromosomes red. Top numbers show time in seconds from NEB. Bars = 10 μm.

Feo inhibition significantly decreased the extent of anaphase B spindle elongation from 4.31 ± 0.76 (29 spindles in six embryos) to 2.27 ±1.03 μm (27 spindles in three embryos; $p = 1.009e\text{-}10$; Figure 2C) and slightly decreased the maximum rate of anaphase B elongation from 0.078 ± 0.019 (36 spindles in seven embryos) to 0.064 ± 0.018 μm/s (56 spindles in eight embryos; $p = 0.003197$). These effects of Feo inhibition were specific to anaphase/telophase, because ~95% of anti-Feo–injected spindles proceeded to anaphase normally (mistimed antibody microinjection during the previous anaphase/telophase led to aberrant metaphase spindle assembly in only 5.5% of spindles analyzed [219 spindles in 27 embryos]). Overall our results agree with those obtained in other *Drosophila*

Feo antibody against high-speed supernatant (HSS) of *Drosophila* embryos. (F) Microinjection of the purified Feo antibody dissociated Feo-GFP from prometaphase (left) and anaphase B (right) spindles. Arrows mark microinjection site. Merged (Feo, green; tubulin, red) and Feo images are shown. Away from the injection site, Feo-GFP faintly localizes to prometaphase spindles (left, arrowheads) and accumulates at the midzone of anaphase B spindles (right, arrowheads). Around the injection site, anti-Feo antibody dissociates Feo-GFP from the spindles and forms immunoprecipitates. Repeated in >20 embryos. See Supplemental Figure S1 for the gradient of spindle phenotypes corresponding to Feo-GFP depletion. Bars, 5 μm.

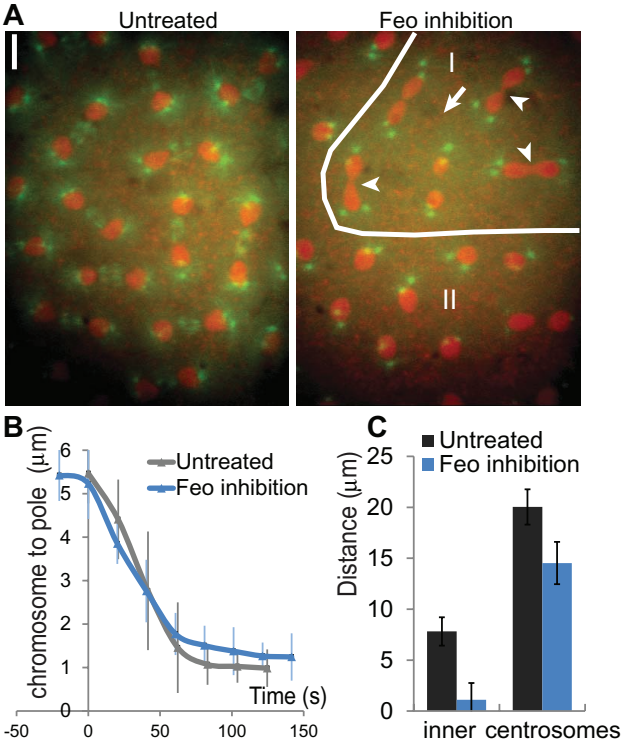

FIGURE 3: Feo inhibition caused defects in chromosome segregation in *Drosophila* embryos. (A) Feo inhibition caused incomplete chromosome segregation, characterized by the presence of chromosome bridges (arrowheads) between the two daughter nuclei even after nuclear envelope re-formation (region I). Away from the injection site, daughter nuclei appear to be properly segregated, but midbodies were not present between them (region II). The arrow shows the injection site. Bar, 10 µm. (B) Chromosome-to-pole distance vs. time in untreated and anti-Feo–injected embryos. 0 s, anaphase A onset. Averages of ≥6 spindles. (C) Distance between the inner edges of daughter nuclei (inner) and between centrosomes (centrosomes) at the end of telophase in untreated and anti-Feo–injected embryos. Twenty-six spindles in two embryos were measured for control (untreated), and 34 spindles in three embryos were measured after Feo inhibition.

cell types, in which the functional disruption of Feo produced thin MT bundles and disorganized central spindles during telophase. It is striking, however, that in those previous studies, no defects in anaphase B spindle elongation were observed (Verni *et al.*, 2004).

Feo is essential for proper chromosome segregation in *Drosophila* embryos

After Feo inhibition, we also observed chromosome segregation defects characterized by the presence of chromosome bridges in 88% of the spindles (59 spindles in six embryos). The chromosome bridges remain present after nuclear envelope re-formation, resulting in daughter nuclei linked by a thin bridge (Figure 3A). We quantified the anaphase A chromosome-to-pole movement in untreated and Feo-inhibited embryos. Feo inhibition caused a slight reduction in anaphase A chromosome-to-pole movement from 0.082 ± 0.10 (18 spindles in two embryos) to 0.067 ± 0.013 µm/s (32 spindles in four embryos; Figure 3B; p = 5.557e-08), but anaphase A chromosome-to-pole movement was complete in all spindles analyzed. Thus the observed defects are unlikely due to defects in anaphase A chromosome-to-pole movement.

At the end of telophase, the distances between centrosomes and between paired nuclei were significantly decreased after Feo inhibition (Figure 3C), suggesting that incomplete pole-pole separation during anaphase B is correlated with the chromosome segregation defects observed after Feo inhibition. Previously we showed that patronin inhibition causes defects in anaphase B spindle elongation, which also led to defects in chromosome segregation (Wang *et al.*, 2013). Both studies underscore the importance of anaphase B spindle elongation for chromosome segregation.

Feo antagonizes the association of kinesin-5 with the anaphase B spindle midzone

We tested the idea that the aforementioned defects in mitosis might reflect the effects of loss of Feo function on the localization of the three primary spindle midzone motors—kinesin-5 (KLP61F), kinesin-4 (KLP3A), and kinesin-6 (PavKLP). Previous work suggested that these motors play critical roles in anaphase B and cytokinesis. Kinesin-5 serves as the primary antiparallel MT-MT sliding motor driving poleward flux and spindle elongation (Sharp *et al.*, 2000; Brust-Mascher *et al.*, 2004, 2009); kinesin-4 somehow contributes to the down-regulation of poleward flux, leading to a corresponding enhancement of spindle elongation (Brust-Mascher *et al.*, 2004; Kwon *et al.*, 2004), and kinesin-6 bundles MTs of the late anaphase/telophase midzone and is required for cleavage furrow assembly and cytokinesis (Adams *et al.*, 1998).

In the case of kinesin-5, as in previous immuno–electron microscopy and live-cell imaging (Sharp *et al.*, 1999; Cheerambathur *et al.*, 2008), in KLP61F-GFP–rescued flies (Cheerambathur *et al.*, 2008), we observed that kinesin-5 colocalizes with tubulin throughout the spindle, is more concentrated around the poles during metaphase and anaphase, and displays a characteristic but previously unexplained narrow dip in fluorescence intensity at the equator during late anaphase B and telophase (Figure 4, A and B). We emphasize, however, that KLP61F is localized all along ipMT bundles through anaphase B, including ipMTs crossing the midzone, where this decrease in intensity occurs and therefore it is appropriately positioned to slide apart antiparallel MTs to drive poleward flux and pole–pole separation in wild-type embryo spindles (Figure 4, A and B). We observed that the dip in KLP61F fluorescence intensity during anaphase B and telophase coincides with the site of Feo accumulation in the center of the midzone (Figure 4A and Supplemental Video S6). We also note that KLP61F is less concentrated at the equator during metaphase, but this reflects steric exclusion by chromosomes at the equator (Figure 4B, bottom).

Surprisingly, after Feo inhibition in KLP61F-GFP rescued flies (Cheerambathur *et al.*, 2008), the distribution of KLP61F is significantly altered from anaphase B on (Figure 4C and Supplemental Videos S7 and S8). KLP61F concentrates at the spindle midzone, and the characteristic dip does not form. Feo inhibition does not affect the distribution of KLP61F during metaphase, suggesting that Feo specifically regulates KLP61F during anaphase B by limiting the amount of KLP61F associated with the center of the antiparallel overlap zone. To explore this further, we compared the KLP61F-to-tubulin ratio in untreated and Feo-inhibited embryos. In the inhibited embryo spindles, this ratio is not affected during metaphase, but it is higher at the midzone from anaphase B on (Figure 4C). Quantification of the KLP61F-to-tubulin ratio at the spindle midzone during metaphase and anaphase B shows that in untreated embryos, the anaphase B ratio is similar to the metaphase ratio, but after Feo inhibition the ratio during anaphase B is significantly increased (Figure 4D). Ase1p and kinesin-5 have a similar preference for cross-linking MTs into antiparallel versus

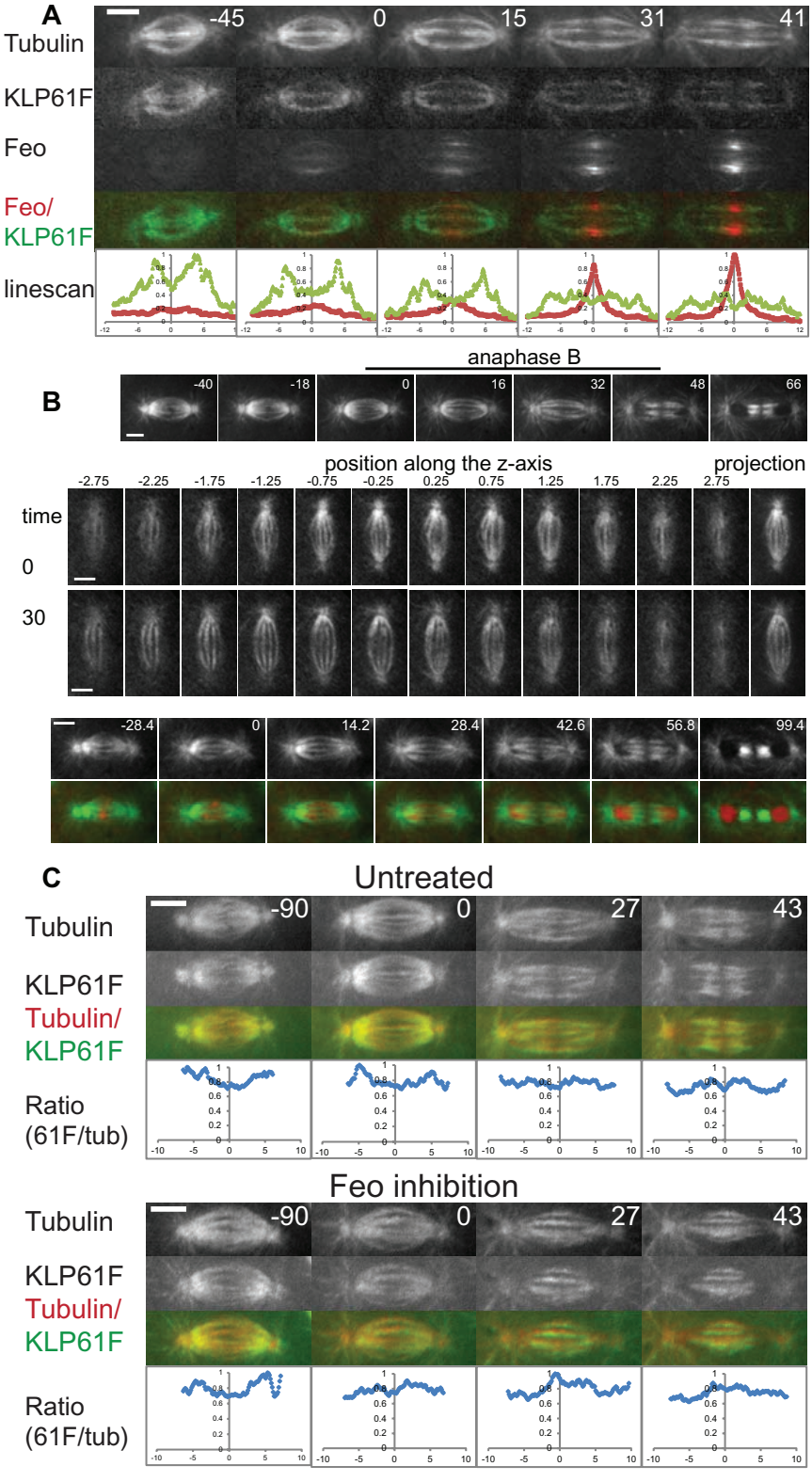

D Normalized Midzone 61F/Tub Ratio

	Untreated	Feo inhibition
Metaphase	1	1
Anaphase B	0.9±0.1	1.4±0.2
spindles/embryos	31/3	37/4

parallel orientations, and therefore we propose that in wild-type embryos, Feo and KLP61F competitively bind to antiparallel MTs, and thus KLP61F replaces antibody-dissociated Feo in bridging antiparallel MTs at the center of the spindle midzone when Feo is absent.

However, kinesin-5 cannot *functionally* substitute for the loss of Feo from the spindle midzone because, as shown, defects in anaphase B spindle elongation clearly occur (Figure 2). Thus it is possible that in wild-type embryos, Feo accumulation at the spindle midzone limits the number of KLP61F motors that associate with midzonal antiparallel ipMTs to somehow optimize their MT-MT sliding activity and also helps to organize antiparallel MTs into an ordered structure that facilitates kinesin-5–driven anaphase B spindle elongation. This effect of Feo in regulating kinesin-5 localization differs from the situation in *Saccharomyces cerevisiae*, in which Ase1p appears to positively regulate the spindle localization of the sliding motors. In the latter case, the kinesin-5, CIN8, must bind to Ase1p in order to associate with the midzone and drive spindle elongation (Khmelinskii *et al.*, 2009).

Feo is required for kinesin-4 accumulation to the spindle midzone during anaphase B and telophase

We next examined the effect of loss of Feo function on the localization of kinesin-4. In mammalian

FIGURE 4: Influence of Feo on the spindle midzone localization of the MT sliding motor, kinesin-5. (A) Dynamics of KLP61F (kinesin-5)-GFP and Feo-mCherry during *Drosophila* embryo mitosis. In the merged images and line scans, Feo is shown in red and KLP61F in green. See Supplemental Video S6. (B) KLP61F localizes all along spindle MTs. Top, time series of a single plane through the center of the spindle; KLP61F-GFP decorates all spindle MTs, the intensity in the center of the midzone decreases during anaphase B, and a gap is clearly visible at telophase. Middle, *Z*-series through a spindle at the onset and the second half of anaphase B. KLP61F clearly labels MTs from pole to pole. Bottom, comparison of KLP61F and chromosome localization. Time 0, anaphase B onset. Bar, 5 μm. (C) Effect of Feo inhibition on the dynamics of KLP61F in *Drosophila* embryo mitosis. The midzone association of kinesin-5 is enhanced during anaphase B after Feo inhibition. Bottom, ratio of KLP61F:tubulin fluorescence intensity. The maximum ratio in all images is set to 1.0 to normalize the data. Repeated in >20 embryos. See Supplemental Videos S7 and S8. (D) KLP61F/tubulin ratio at the spindle midzone during metaphase and anaphase B in untreated and Feo-inhibited embryos. The KLP61F/tubulin ratio during anaphase was normalized with the ratio during metaphase. The number of spindles/embryos analyzed is shown at the bottom. $p < 2.2e\text{-}16$. Bars, 5 μm.

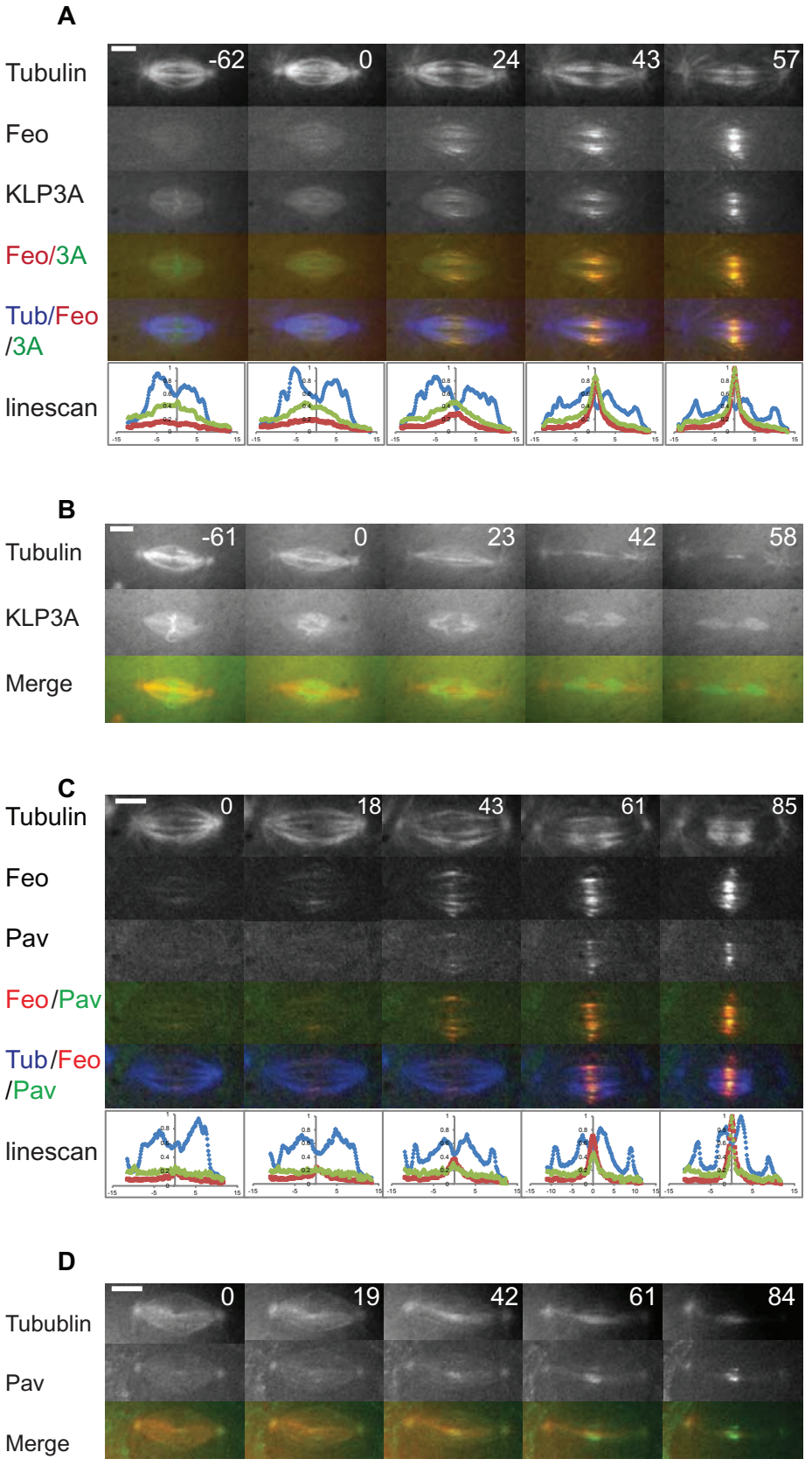

FIGURE 5: Influence of Feo on the spindle midzone localization of the MT motors, kinesin-4 and kinesin-6. (A) Dynamics of KLP3A (kinesin-4)-GFP and Feo-mCherry during *Drosophila* embryo mitosis. In the merged images and line scans, Feo is shown in red, KLP3A in green, and tubulin in blue. See Supplemental Videos S9 and S10. (B) Effect of Feo inhibition on the dynamics of KLP3A during anaphase B and telophase (compare with A). Repeated in 12 embryos. (C) Dynamics of Pav (kinesin-6)-GFP and Feo-mCherry during mitosis. In the merged images and line scans, Feo is shown in red, Pav in green, and tubulin in blue. See Supplemental Videos S11 and S12. (D) Effect of Feo inhibition on the dynamics of Pav-GFP during anaphase B and telophase (compare with C). Repeated in six embryos. Bars, 5 μm. 0 s, anaphase B onset.

cells, PRC1 is required for localization of kinesin-4, and direct interaction between Feo and kinesin-4 has been reported in *Drosophila* S2 cells (D'Avino *et al.*, 2007). To test whether Feo is required to target the *Drosophila* kinesin-4 KLP3A to the spindle midzone, we compared the dynamics of both proteins (Figure 5A) and examined how the loss of Feo function affects the dynamics of KLP3A-GFP during mitosis (Figure 5B). Consistent with previous immunostaining (Kwon *et al.*, 2004), in wild-type embryos, KLP3A-GFP concentrated on chromosomes and only weakly localized to spindle MTs during metaphase, but during anaphase and telophase, KLP3A-GFP dissociated from the chromosomes and concentrated on the spindle midzone, displaying strong colocalization with Feo (Figure 5A and Supplemental Videos S9 and S10). After Feo inhibition, however, KLP3A localized normally to metaphase chromosomes but did not translocate to the midzone, instead remaining associated with chromosomes throughout anaphase B and telophase (Figure 5B). This suggests that Feo targets KLP3A to the anaphase spindle midzone, in agreement with previous data showing that the midzone localizations of PRC1 and KIF4 are interdependent in mammalian cells (Kurasawa *et al.*, 2004; Zhu and Jiang, 2005). The midzone defects resulting from Feo inhibition (Figure 2) are not solely due to failures in KLP3A targeting, because in KLP3A-inhibited embryos, midzones splay out into broader structures than those in controls (Kwon *et al.*, 2004), whereas in Feo-inhibited embryos, midzones become narrower. Thus the midzone defects observed after Feo inhibition are a direct result of loss of Feo-dependent midzonal MT bundling.

Feo inhibition does not influence kinesin-6 localization to the spindle midzone

Feo does not seem to influence the association of PavKLP with the spindle midzone; in wild-type embryos, PavKLP accumulated to a narrower region of the midzone than Feo (Figure 5C and Supplemental Videos S11 and S12) and retained

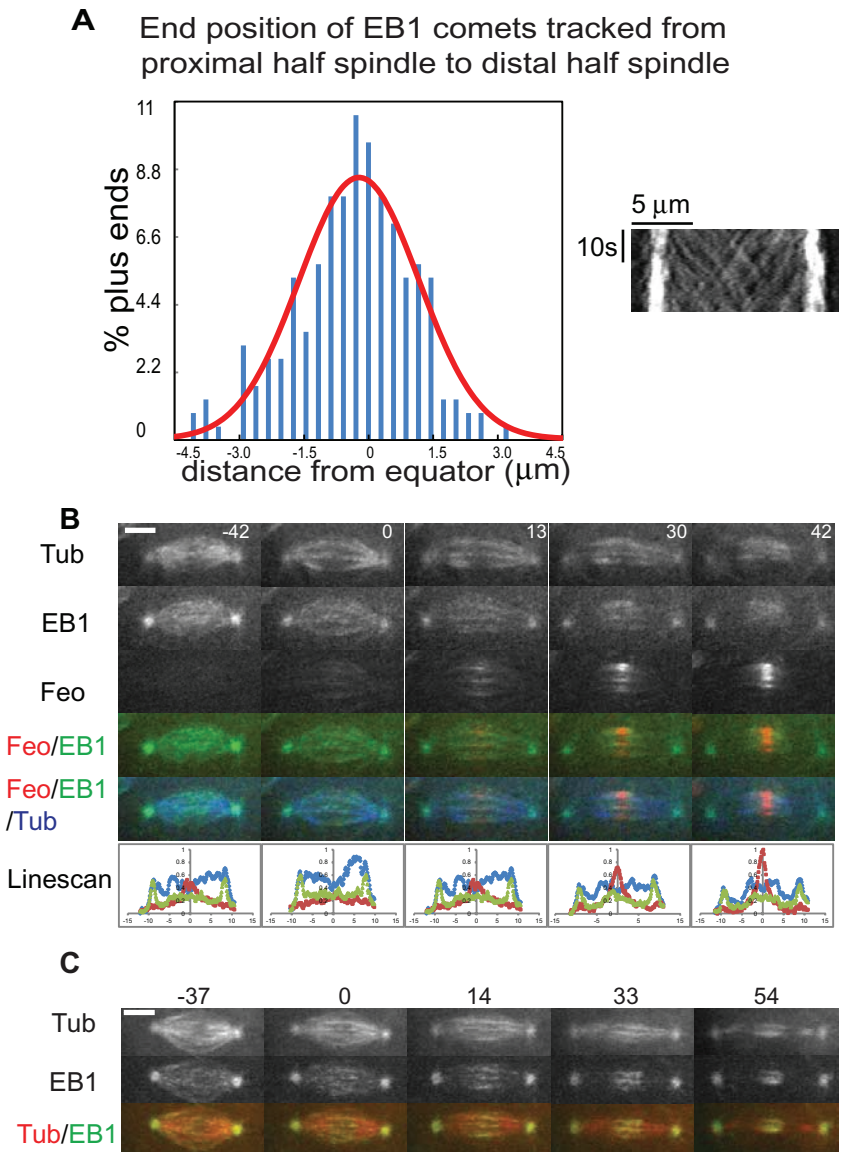

FIGURE 6: Effect of Feo inhibition on MT plus end dynamics. (A) Histogram of the distribution of EB1 comet excursions into the distal half-spindle measured from spindle equator (0 µm). Example EB1 kymograph. (B) EB1-GFP and Feo-mCherry during mitosis. In the merged images and line scans, Feo is shown in red, EB1 in green, and tubulin in blue. (C) Feo inhibition does not affect the redistribution of EB1 at anaphase B onset. Bars, 5 µm.

this localization after Feo inhibition (Figure 5D). This is consistent with previous work in S2 cells (D'Avino *et al.*, 2007), but differs from results showing that loss of Feo activity in spindles of other *Drosophila* cell types leads to the mislocalization of this kinesin-6 during telophase and to defects in cytokinesis (Verni *et al.*, 2004). In addition, in *Schizosaccharomyces pombe*, Ase1p recruits the kinesin-6, klp9p, to the spindle midzone, where this motor drives anaphase B spindle elongation (Fu *et al.*, 2009).

Feo inhibition has no effect on the redistribution of ipMT plus ends at anaphase B onset

Ase1p/PRC1 family members and their associated proteins (e.g., kinesin-4, Bieling *et al.*, 2010; CLASP1, Liu *et al.*, 2009) have been reported to be involved in regulating MT plus end dynamics. We tested whether Feo has a role in the redistribution of MT plus ends observed at anaphase B onset (Cheerambathur *et al.*, 2007) by injecting Feo antibody into flies expressing EB1-GFP, a marker of growing MT plus ends (Figure 6A). After Feo inhibition, spindles were narrower, but EB1-GFP still redistributed to the spindle midzone at anaphase B onset (Figure 6, B vs. C). Given that the midzone localization of kinesin-4 was abolished after Feo inhibition, our observation that Feo inhibition has no effect on EB1 concentration at anaphase B onset suggests that neither Feo nor kinesin-4 at the midzone is responsible for the redistribution of MT plus ends at anaphase B onset.

Feo and kinesin-5 display different patterns of localization along antiparallel MTs in the anaphase B spindle midzone

Our functional data suggest that kinesin-5 and Feo cooperate at the spindle midzone to produce the robust anaphase B spindle elongation and faithful chromosome segregation observed in wild-type embryo spindles. To estimate their relative distribution on antiparallel ipMTs at the midzone, we evaluated the maximal size of the zone of overlapping MTs by tracking EB1-GFP in living transgenic embryos and measuring the excursions of growing MT plus ends that move across the equator from one half-spindle to the opposite half-spindle. These measurements suggest a midzone length of ~3–4 µm (Figures 6A and 7A). During anaphase B, Feo is localized in a tight band at the center of the overlap zone marked by EB1 (Figures 6B and 7A), where it could organize adjacent antiparallel MTs into bundles with optimal spacing. Kinesin-5 is distributed mainly along midzonal antiparallel ipMTs adjacent to this Feo zone (Figure 7A), where it could slide apart optimally spaced MTs, supporting the hypothesis that Feo partially restricts the association of kinesin-5 with the center of the midzone, possibly by steric inhibition as a result of its being assembled into a dense, multimeric midzone matrix (Schuyler *et al.*, 2003; Kapitein *et al.*, 2008; Hutterer *et al.*, 2009). An accurate picture of the distribution of overlapping MTs and associated proteins at the midzone would require high-resolution studies (e.g., multiple-label immuno–electron microscopy; Sharp *et al.*, 1999), but our light microscopy data (Figure 7A) support the model shown in the cartoon in Figure 7B.

DISCUSSION

The spindle midzone appears to be a conserved structure overall, containing common molecular components that associate with its dense network of antiparallel MTs (Glotzer, 2009; Peterman and Scholey, 2009; Mitchison *et al.*, 2013). However, current and previous studies suggest that these components display system-specific variations in their interactions, targeting, and functions, conforming to the general idea that the mitotic spindle consists of conserved

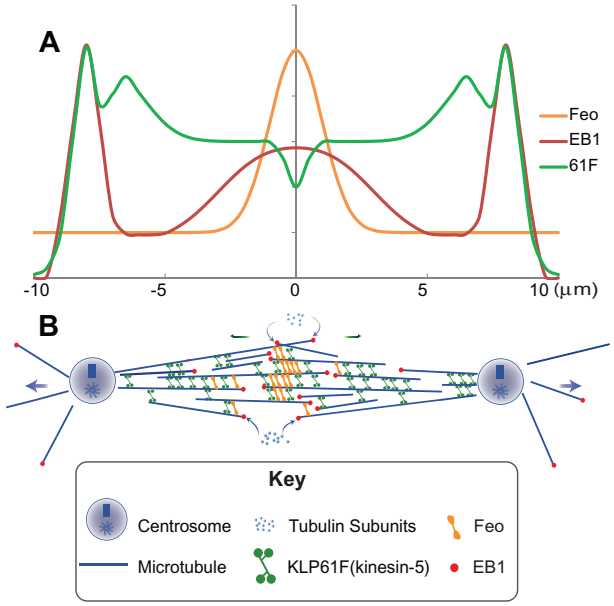

FIGURE 7: Model for the functional interaction between Feo and kinesin-5 on antiparallel ipMTs at the spindle midzone during anaphase B in *Drosophila* embryos. (A) Diagrammatic representation of the relative distributions of Feo, EB1, and KLP61F along the anaphase B spindle. Center (0), spindle equator. Vertical axis shows relative fluorescence intensity (1 is maximum for each protein). (B) Model of the anaphase B spindle midzone showing the spatial relationship between Feo, EB1, and KLP61F. Feo preferentially bundles antiparallel ipMTs and also localizes weakly to parallel MTs. EB1, a marker of growing MT plus ends, is concentrated at the midzone. KLP61F cross-links parallel and antiparallel MTs and slides apart antiparallel ipMTs. The kinesin-5–driven antiparallel ipMT sliding requires Feo-mediated midzone organization to produce normal anaphase B spindle elongation.

molecules and biochemical modules that are deployed in a system-specific, combinatorial manner (Goshima and Scholey, 2010). The role of the key Ase1p family member, PRC1/Feo, appears to differ in different systems. In this study, we focused on its role in *Drosophila* syncytial embryo mitosis.

Previous work on Feo in *Drosophila* was based on fixed immunostaining data and focused on the role of Feo in organizing the spindle midzone during telophase and cytokinesis. Here we characterized the real-time dynamics of Feo and its interactions with key MT-MT cross-linking motors and uncovered an essential role for Feo in anaphase B spindle elongation and chromosome segregation. Using the *Drosophila* syncytial embryo, in which rounds of mitosis occur very rapidly without intervening cytokinesis, our work revealed the roles of Feo during late mitosis. Thus, in contrast to previous studies (Verni *et al.*, 2004), we show that Feo inhibition caused significant defects in anaphase B spindle elongation and midzone assembly, which lead to defects in chromosome segregation and telophase midbody structure.

To our knowledge, this is the first time that an Ase1p family member has been shown to contribute to anaphase B spindle elongation in metazoan systems. Of interest, the mechanism by which Feo contributes to anaphase B spindle elongation seems to differ from the role of Ase1p in yeast. Whereas Ase1p recruits sliding motors (kinesin-5 or kinesin-6) to the spindle midzone to initiate anaphase B spindle elongation in yeast (Khmelinskii *et al.*, 2009), in *Drosophila* embryos, Feo appears to restrict the association of the sliding motor, kinesin-5, to the spindle midzone. *Drosophila* embryo spindle midzones contain a single type of kinesin-5, kinesin-4, and kinesin-6, whereas *S. cerevisiae* spindles use two distinct types of kinesin-5 motors, but no kinesin-4 or kinesin-6 is present (Saunders and Hoyt, 1992; Straight *et al.*, 1998). Whereas kinesin-5 appears to be the primary motor at the spindle midzone driving anaphase B in *Drosophila* embryo and *S. cerevisiae* mitotic spindles (Straight *et al.*, 1998; Brust-Mascher *et al.*, 2009), kinesin-6 fulfills this role in *S. pombe* (Fu *et al.*, 2009). We find that the midzone association of Feo is not required for the association of kinesin-6 with the *Drosophila* embryo mitotic spindle midzone, consistent with results in mammalian cells but different from the situation in *S. pombe*, where Ase1p is required for kinesin-6 localization (Kurasawa *et al.*, 2004; Fu *et al.*, 2009).

In many systems, including *Drosophila* S2 cells, members of the Ase1p family have been shown to directly interact with kinesin-4 during late mitosis (Kurasawa *et al.*, 2004; Zhu and Jiang, 2005; D'Avino *et al.*, 2007). In the present study, we show that Feo is required for the translocation of *Drosophila* kinesin-4, KLP3A, from chromosomes to the spindle midzone during anaphase B and telophase and that accumulation and colocalization of Feo and KLP3A to the anaphase B spindle midzone are regulated by cyclin B degradation and cdk1 inactivation, as shown in mammalian cells (Kurasawa *et al.*, 2004; Zhu *et al.*, 2006). In S2 cells, the interaction between *Drosophila* Feo and KLP3A depends on their phosphorylation states (D'Avino *et al.*, 2007), and it has also been shown that PRC1 is directly phosphorylated by cdk1 in early mitosis and that its dephosphorylation may increase its affinity for MTs (Zhu and Jiang, 2005; Zhu *et al.*, 2006; Subramanian *et al.*, 2013). It is therefore possible that in *Drosophila* embryos, in response to cyclin B degradation and cdk1 inactivation, dephosphorylated Feo increases its binding affinity to MTs and KLP3A and thus recruits KLP3A to the antiparallel overlap to organize the anaphase B spindle midzone. Of note, both Feo and KLP3A inhibition destabilize ipMTs and cause defects in anaphase B spindle elongation; however, KLP3A inhibition causes disorganized "splayed" MTs with an increased spindle width-to-length ratio during anaphase B (Kwon *et al.*, 2004), whereas Feo inhibition causes a narrower and denser spindle midzone, suggesting that in addition to recruiting KLP3A, Feo has independent roles in the organization of the anaphase B spindle midzone.

The present study illuminates the key role of Feo in assembling and organizing the spindle midzone. Our results suggest that Feo localization to the spindle midzone from early anaphase on is required to allow the key MT sliding motor, kinesin-5, to drive normal anaphase B spindle elongation. Consequently, after its antibody-induced dissociation, only a narrow midzone can assemble, leading to a reduced rate and extent of spindle elongation. However, while Feo is required for kinesin-5–driven anaphase B spindle elongation, it does not appear to be required for kinesin-5–driven poleward flux during pre–anaphase B because it does not start to accumulate on the spindle midzone until anaphase B onset. Members of the kinesin-5 family of motors and the Ase1p family of nonmotor MAPs both localize to antiparallel ipMTs of the anaphase B spindle midzone in fly embryo spindles, and they share a similar preference for cross-linking MTs into antiparallel versus parallel polarity patterns in vitro. It is striking that kinesin-5 localization to the embryo spindle midzone increases when Feo is depleted, yet the additional kinesin-5 cannot substitute for the decrease in Feo function despite sharing its antiparallel MT cross-linking activity. This suggests that Feo-dependent assembly and organization of the midzone is required for proper anaphase B spindle elongation, probably by organizing antiparallel

ipMTs into properly spaced networks containing the appropriate number of kinesin-5 motors consistent with optimal outward sliding of the ipMTs, which drive pole–pole separation (Lansky *et al.*, 2015). We propose that these cell cycle–regulated Feo and kinesin-5–dependent midzone-associated processes (Cheerambathur *et al.*, 2007; Bastos *et al.*, 2014) cooperate with events at the spindle pole, where, after cyclin B degradation, patronin-mediated suppression of kinesin-13 activity converts MT poleward flux into anaphase B spindle elongation (Wang *et al.*, 2013). Finally, we note that the frequency of anaphase B errors that accompany aging in humans has been associated with an increased risk of cancer (Ford, 2013), suggesting that these processes may be medically relevant.

MATERIALS AND METHODS

Generation of transgenic flies

For Feo-mCherry transgenic flies, a full-length Feo (fascetto) cDNA was subcloned with an mCherry coding sequence into the pWR-pUbq vector (provided by N. Brown, University of Cambridge, Cambridge, United Kingdom) downstream of the polyubiquitin promoter (Wang *et al.*, 2013), and the resulting transgenic flies with a single insertion in the third chromosome were generated by BestGene (Chino Hills, CA). For KLP3A-GFP transgenic flies, a cDNA encoding full-length KLP3A (provided by Michael Goldberg, Cornell University, Ithaca, NY; Kwon *et al.*, 2004) was subcloned with a GFP coding sequence into the pWR-pUbq vector in a similar way, and the resulting transgenic flies with a single insertion in the X chromosome were generated by BestGene.

Drosophila stocks and embryo preparation

All flies were maintained at 25°C. Transgenic flies coexpressing GFP-tubulin and RFP-histone were generated as described (Wang *et al.*, 2013). Flies with an EB1-GFP (Cheerambathur *et al.*, 2007), KLP61F-GFP (Cheerambathur *et al.*, 2008), PavKLP-GFP (Sommi *et al.*, 2011), or Feo-GFP transgene (Wang *et al.*, 2013) were expressed as previously described. Flies expressing Polo-GFP were kindly provided by Claudio Sunkel (Institute for Molecular and Cell Biology, University of Porto, Porto, Portugal). Flies coexpressing Feo-mCherry and KLP3A-GFP or KLP61F-GFP or PavKLP-GFP or EB1-GFP were generated by standard crossing. Embryos were prepared as described (Wang *et al.*, 2013).

Protein purification, antibody generation, and microinjection

Embryos were premicroinjected with rhodamine-labeled tubulin or HiLyte Fluor 647–labeled tubulin (Cytoskeleton, Denver, CO) when necessary to visualize tubulin. GST-cyclin B was purified as described (Cheerambathur *et al.*, 2007). Anti-Feo antibody was affinity purified with GST-tagged Feo N-terminal fragments (amino acids 1–250 and 1–480) from a rabbit anti-Feo serum against histidine-tagged full-length Feo protein. To purify wild-type full-length Feo protein, Feo cDNA was cloned into pFastBac HTc vector (Invitrogen, Carlsbad, CA) and then expressed in baculovirus system and purified with Ni-nitriloacetic acid agarose (Qiagen, Valencia, CA). All injected proteins were dialyzed in phosphate-buffered saline (PBS) and concentrated before injection.

Most embryos were injected with anti-Feo antibody in interphase of cycle 10 or 11 and imaged in the following cycle. Embryos were injected with cdk1 inhibitor (purvalanol, injection concentration 100 mM) and cyclin B at the indicated time and immediately imaged after microinjection. All shown spindles, except those within a gradient, were within 50 µm of the injection site, and the injection site was determined by approximate eye observation and confirmed by the most severe phenotypes. In figures showing a gradient of effects (Figures 1F, 2A, and 3A), the injection sites are shown by arrows in the first frame. The average intracellular concentration was calculated as protein concentration times the estimated injection volume/embryo volume and is ~0.5 mg/ml for anti-Feo antibody and ~0.3 mg/ml for cyclin B.

Time-lapse and fluorescence microscopy and statistical analysis

Time-lapse images were acquired on an inverted microscope (IX-70; Olympus, Tokyo, Japan) equipped with an UltraView spinning-disk confocal head (PerkinElmer-Cetus, Waltham, MA), a UPlan Apochromat 100× 1.35 numerical aperture (NA) or Plan-Apochrom at 60× 1.4 NA oil immersion objective, and an Orca ER charge-coupled device camera (Hamamatsu, Hamamatsu, Japan) using Volocity software (PerkinElmer-Cetus). Either a single confocal plane or a stack of 11 planes spaced by 0.5 µm was acquired at time intervals of 0.5–28 s at room temperature.

Images were analyzed with MetaMorph software (Universal Imaging, West Chester, PA) as described (Brust-Mascher *et al.*, 2009). Pole and chromosome leading-edge positions were logged in each image. Pole-to-pole and chromosome-to-pole distances as functions of time were calculated from these positions. Anaphase A and anaphase B rates were measured as the maximum linear rates. Calculations were performed on Excel (Microsoft, Redmond, WA). All value comparisons were performed using the Wilcoxon rank sum test on R (www.r-project.org/). All error bars shown in the figures are SDs.

Line scans were obtained with the MetaMorph LineScan function. To calculate the relative fluorescence intensity in the line scans, the minimum fluorescence intensity in the line scans from all images was set to 0, and the maximum fluorescence intensity was set to 1.0, unless otherwise specified.

To quantify the ratio of fluorescent protein to tubulin in each spindle (Figure 4D and Supplemental Figure S1C), embryos were preinjected with rhodamine-tubulin at least 1 h before imaging to allow even distribution. We measured the intensity of GFP and of rhodamine in the spindle midzone, subtracted background fluorescence intensity, and ratioed these two values.

Note added in proof. While this paper was in press, Lansky *et al.*, 2015, reported that yeast Ase1p can generate entropic forces to direct MT sliding. It will be interesting to test whether such forces generated by Feo can cooperate with kinesin-5–mediated ipMT sliding forces to contribute to anaphase B spindle elongation.

ACKNOWLEDGMENTS

This project was supported by National Institutes of Health Grant GM55507 to J.M.S. We thank Li Tao for help in purifying the full-length Feo protein and Maurizio Gatti for useful discussion.

REFERENCES

Acar S, Carlson DB, Budamagunta MS, Yarov-Yarovoy V, Correia JJ, Ninonuevo MR, Jia W, Tao L, Leary JA, Voss JC, *et al.* (2013). The bipolar assembly domain of the mitotic motor kinesin-5. Nat Commun 4, 1343.

Adams RR, Tavares AA, Salzberg A, Bellen HJ, Glover DM (1998). pavarotti encodes a kinesin-like protein required to organize the central spindle and contractile ring for cytokinesis. Genes Dev 12, 1483–1494.

Bastos RN, Cundell MJ, Barr FA (2014). KIF4A and PP2A-B56 form a spatially restricted feedback loop opposing Aurora B at the anaphase central spindle. J Cell Biol 207, 683–693.

Bieling P, Telley IA, Surrey T (2010). A minimal midzone protein module controls formation and length of antiparallel microtubule overlaps. Cell 142, 420–432.

Brust-Mascher I, Civelekoglu-Scholey G, Kwon M, Mogilner A, Scholey JM (2004). Model for anaphase B: role of three mitotic motors in a switch from poleward flux to spindle elongation. Proc Natl Acad Sci USA 101, 15938–15943.
Brust-Mascher I, Scholey JM (2002). Microtubule flux and sliding in mitotic spindles of Drosophila embryos. Mol Biol Cell 13, 3967–3975.
Brust-Mascher I, Scholey JM (2011). Mitotic motors and chromosome segregation: the mechanism of anaphase B. Biochem Soc Trans 39, 1149–1153.
Brust-Mascher I, Sommi P, Cheerambathur DK, Scholey JM (2009). Kinesin-5-dependent poleward flux and spindle length control in Drosophila embryo mitosis. Mol Biol Cell 20, 1749–1762.
Cheerambathur DK, Brust-Mascher I, Civelekoglu-Scholey G, Scholey JM (2008). Dynamic partitioning of mitotic kinesin-5 cross-linkers between microtubule-bound and freely diffusing states. J Cell Biol 182, 429–436.
Cheerambathur DK, Civelekoglu-Scholey G, Brust-Mascher I, Sommi P, Mogilner A, Scholey JM (2007). Quantitative analysis of an anaphase B switch: predicted role for a microtubule catastrophe gradient. J Cell Biol 177, 995–1004.
Civelekoglu-Scholey G, Cimini D (2014). Modelling chromosome dynamics in mitosis: a historical perspective on models of metaphase and anaphase in eukaryotic cells. Interface Focus 4, 20130073.
Cole DG, Saxton WM, Sheehan KB, Scholey JM (1994). A "slow" homotetrameric kinesin-related motor protein purified from Drosophila embryos. J Biol Chem 269, 22913–22916.
D'Avino PP, Archambault V, Przewloka MR, Zhang W, Lilley KS, Laue E, Glover DM (2007). Recruitment of Polo kinase to the spindle midzone during cytokinesis requires the Feo/Klp3A complex. PLoS One 2, e572.
Duellberg C, Fourniol FJ, Maurer SP, Roostalu J, Surrey T (2013). End-binding proteins and Ase1/PRC1 define local functionality of structurally distinct parts of the microtubule cytoskeleton. Trends Cell Biol 23, 54–63.
Ford JH (2013). Protraction of anaphase B in lymphocyte mitosis with ageing: possible contribution to age-related cancer risk. Mutagenesis 28, 307–314.
Fu C, Ward JJ, Loiodice I, Velve-Casquillas G, Nedelec FJ, Tran PT (2009). Phospho-regulated interaction between kinesin-6 Klp9p and microtubule bundler Ase1p promotes spindle elongation. Dev Cell 17, 257–267.
Gadde S, Heald R (2004). Mechanisms and molecules of the mitotic spindle. Curr Biol 14, R797–R805.
Gerdes K, Howard M, Szardenings F (2010). Pushing and pulling in prokaryotic DNA segregation. Cell 141, 927–942.
Glotzer M (2009). The 3Ms of central spindle assembly: microtubules, motors and MAPs. Nature reviews. Mol Cell Biol 10, 9–20.
Goodwin SS, Vale RD (2010). Patronin regulates the microtubule network by protecting microtubule minus ends. Cell 143, 263–274.
Goshima G, Scholey JM (2010). Control of mitotic spindle length. Annu Rev Cell Dev Biol 26, 21–57.
Hayward D, Metz J, Pellacani C, Wakefield JG (2014). Synergy between multiple microtubule-generating pathways confers robustness to centrosome-driven mitotic spindle formation. Dev Cell 28, 81–93.
Helmke KJ, Heald R, Wilbur JD (2013). Interplay between spindle architecture and function. Int Rev Cell Mol Biol 306, 83–125.
Hu CK, Ozlu N, Coughlin M, Steen JJ, Mitchison TJ (2012). Plk1 negatively regulates PRC1 to prevent premature midzone formation before cytokinesis. Mol Biol Cell 23, 2702–2711.
Hutterer A, Glotzer M, Mishima M (2009). Clustering of centralspindlin is essential for its accumulation to the central spindle and the midbody. Curr Biol 19, 2043–2049.
Kapitein LC, Janson ME, van den Wildenberg SM, Hoogenraad CC, Schmidt CF, Peterman EJ (2008). Microtubule-driven multimerization recruits ase1p onto overlapping microtubules. Curr Biol 18, 1713–1717.
Kashina AS, Baskin RJ, Cole DG, Wedaman KP, Saxton WM, Scholey JM (1996). A bipolar kinesin. Nature 379, 270–272.
Khmelinskii A, Roostalu J, Roque H, Antony C, Schiebel E (2009). Phosphorylation-dependent protein interactions at the spindle midzone mediate cell cycle regulation of spindle elongation. Dev Cell 17, 244–256.
Kurasawa Y, Earnshaw WC, Mochizuki Y, Dohmae N, Todokoro K (2004). Essential roles of KIF4 and its binding partner PRC1 in organized central spindle midzone formation. EMBO J 23, 3237–3248.
Kwon M, Morales-Mulia S, Brust-Mascher I, Rogers GC, Sharp DJ, Scholey JM (2004). The chromokinesin, KLP3A, dives mitotic spindle pole separation during prometaphase and anaphase and facilitates chromatid motility. Mol Biol Cell 15, 219–233.
Lansky Z, Braun M, Lüdecke A, Schlierf M, Ten Wolde PR, Janson ME, Diez S (2015). Diffusible crosslinkers generate directed forces in microtubule networks. Cell 160, 1159–1168.
Liu J, Wang Z, Jiang K, Zhang L, Zhao L, Hua S, Yan F, Yang Y, Wang D, Fu C, *et al.* (2009). PRC1 cooperates with CLASP1 to organize central spindle plasticity in mitosis. J Biol Chem 284, 23059–23071.
Maddox P, Desai A, Oegema K, Mitchison TJ, Salmon ED (2002). Poleward microtubule flux is a major component of spindle dynamics and anaphase a in mitotic Drosophila embryos. Curr Biol 12, 1670–1674.
McIntosh JR, Molodtsov MI, Ataullakhanov FI (2012). Biophysics of mitosis. Q Rev Biophys 45, 147–207.
Mitchison TJ, Nguyen P, Coughlin M, Groen AC (2013). Self-organization of stabilized microtubules by both spindle and midzone mechanisms in Xenopus egg cytosol. Mol Biol Cell 24, 1559–1573.
Peterman EJ, Scholey JM (2009). Mitotic microtubule crosslinkers: insights from mechanistic studies. Curr Biol 19, R1089–1094.
Rogers GC, Rogers SL, Schwimmer TA, Ems-McClung SC, Walczak CE, Vale RD, Scholey JM, Sharp DJ (2004). Two mitotic kinesins cooperate to drive sister chromatid separation during anaphase. Nature 427, 364–370.
Saunders WS, Hoyt MA (1992). Kinesin-related proteins required for structural integrity of the mitotic spindle. Cell 70, 451–458.
Scholey JE, Nithianantham S, Scholey JM, Al-Bassam J (2014). Structural basis for the assembly of the mitotic motor Kinesin-5 into bipolar tetramers. Elife 3, e02217.
Schuyler SC, Liu JY, Pellman D (2003). The molecular function of Ase1p: evidence for a MAP-dependent midzone-specific spindle matrix. Microtubule-associated proteins. J Cell Biol 160, 517–528.
Sharp DJ, Brown HM, Kwon M, Rogers GC, Holland G, Scholey JM (2000). Functional coordination of three mitotic motors in Drosophila embryos. Mol Biol Cell 11, 241–253.
Sharp DJ, McDonald KL, Brown HM, Matthies HJ, Walczak C, Vale RD, Mitchison TJ, Scholey JM (1999). The bipolar kinesin, KLP61F, cross-links microtubules within interpolar microtubule bundles of Drosophila embryonic mitotic spindles. J Cell Biol 144, 125–138.
Sommi P, Cheerambathur D, Brust-Mascher I, Mogilner A (2011). Actomyosin-dependent cortical dynamics contributes to the prophase force-balance in the early Drosophila embryo. PLoS One 6, e18366.
Straight AF, Sedat JW, Murray AW (1998). Time-lapse microscopy reveals unique roles for kinesins during anaphase in budding yeast. J Cell Biol 143, 687–694.
Subramanian R, Ti SC, Tan L, Darst SA, Kapoor TM (2013). Marking and measuring single microtubules by PRC1 and kinesin-4. Cell 154, 377–390.
van den Wildenberg SM, Tao L, Kapitein LC, Schmidt CF, Scholey JM, Peterman EJ (2008). The homotetrameric kinesin-5 KLP61F preferentially crosslinks microtubules into antiparallel orientations. Curr Biol 18, 1860–1864.
Verni F, Somma MP, Gunsalus KC, Bonaccorsi S, Belloni G, Goldberg ML, Gatti M (2004). Feo, the Drosophila homolog of PRC1, is required for central-spindle formation and cytokinesis. Curr Biol 14, 1569–1575.
Walczak CE, Cai S, Khodjakov A (2010). Mechanisms of chromosome behaviour during mitosis. Nat Rev Mol Cell Biol 11, 91–102.
Wang H, Brust-Mascher I, Civelekoglu-Scholey G, Scholey JM (2013). Patronin mediates a switch from kinesin-13-dependent poleward flux to anaphase B spindle elongation. J Cell Biol 203, 35–46.
Zheng Y (2010). A membranous spindle matrix orchestrates cell division. Nat Rev Mol Cell Biol 11, 529–535.
Zhu C, Jiang W (2005). Cell cycle-dependent translocation of PRC1 on the spindle by Kif4 is essential for midzone formation and cytokinesis. Proc Natl Acad Sci USA 102, 343–348.
Zhu C, Lau E, Schwarzenbacher R, Bossy-Wetzel E, Jiang W (2006). Spatiotemporal control of spindle midzone formation by PRC1 in human cells. Proc Natl Acad Sci USA 103, 6196–6201.